Chapter 12
Applications of MoS_2 Nanostructures in Wastewater Treatment

Rashi Gusain, Neeraj Kumar, and Suprakas Sinha Ray

Abstract The fascinating properties of two-dimensional (2D) nanomaterial, such as excellent mechanical strength, a high portion of active sites, ease of functionalization and tuning the physical and chemical characteristics, are attracting researchers to host their applications in various fields, including wastewater treatment. Among various 2D nanomaterials, 2D MoS_2 has stand out as a promising alternative inorganic analogue of most explored 2D graphene due to its unique characteristics such as high active surface area, low cost, excellent mechanical strength, small band gap and the possibility of surface functionalization. The excellent water remediation characteristics are attributed to the controlled morphology, specific nano-sized properties, abundant availability, and variable surface chemistry of MoS_2 nanomaterials. Additionally, the selectivity of MoS_2 towards water contaminants promotes its application in water purification. This chapter presents the recent progress, future prospects and challenges of 2D MoS_2-based nanomaterials in water remediation techniques such as adsorbent, photocatalyst, membrane and antibacterial agent. The mechanism behind the water treatment process using 2D MoS_2 is also explained. This chapter will provide a platform to the researchers, who are focused on exploring the application of MoS_2-based materials in water purification. The research demands for future water applications of 2D MoS_2 nanomaterials are also identified.

R. Gusain (✉) · N. Kumar · S. S. Ray
Department of Chemical Sciences, University of Johannesburg, Doornfontein 2028, South Africa
e-mail: dr.rashi20@gmail.com

S. S. Ray
e-mail: rsuprakas@csir.co.za

Centre for Nanostructures and Advanced Materials, DSI-CSIR Nanotechnology Innovation Centre, Council for Scientific and Industrial Research, Pretoria 0001, South Africa

N. Kumar et al. (eds.), *Two-Dimensional Materials for Environmental Applications*, Springer Series in Materials Science 332, https://doi.org/10.1007/978-3-031-28756-5_12

12.1 Introduction

To improve the healthy and ever-lasting qualitative life on the planet, the topmost priority is balancing environmental sustainability. The word environmental sustainability signifies the healthy equilibrium between the consumerist living creatures, especially humans and the living world or the resources of the living world. However, the ever-increasing population, industrialization and urbanization demand more resources and manufacturing for consumption, leading to deforestation, greenhouse gases emission and more energy utilization. This has now become an immense challenge threatening the sustainability of our global society, mainly in the form of the scarcity of freshwater availability, energy supply and climate change. The inadequate supply of clean, fresh water is one of the global challenges which should be concerned for survival and gain the attention of social workers and researchers. Although 70% of the Earth is occupied with water in the form of glaciers, oceans, icecaps, sea, rivers, and lakes, out of all that, only 3% is available for consumption as fresh, clean water, and the rest 97% is salty water, which needs to be treated before any use [1]. Also, untreated effluents from various sources (e.g. domestic, mining, industry, agriculture, pharmaceutical (Fig. 12.1), enter into the freshwater reservoirs and groundwater to take participate in water pollution, which directly/indirectly is dangerous for the human, animals and marine creatures and disturb the sustainability of the life on the planet.

Africa and Asia are the two most affected continents, which will soon run out of clean water for consumption. Therefore, significant efforts are made in water conservation and removing the toxic contaminants from wastewater effluents before discharging them into the water reservoirs or for consumption. The effluents of wastewater contain a wide range of toxic organic (dyes, pharmaceutical by-products and ingredients, pesticides, surfactants, polyaromatic hydrocarbons,

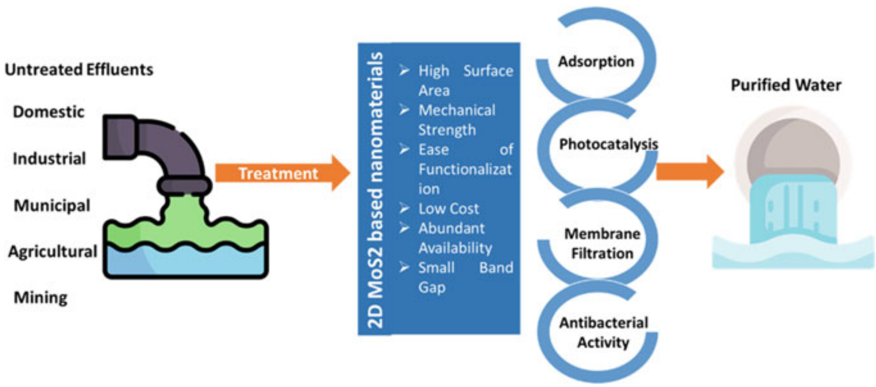

Fig. 12.1 Sources of Wastewater Effluents, properties of MoS_2-based nanomaterials and several wastewater treatment technologies using MoS_2-based nanomaterials

fertilizers, phenols, etc.) and inorganic (mining waste, heavy metal ions, radioactive substances, salts, metal oxides and metal complexes) water contaminants which are a major threat for the eco-system [2]. These toxic water contaminants can be carcinogenic and cause dysfunctional reproductive and immune systems, congenital disabilities, and risk to the physical and mental growth of infants/children [3]. The adverse impact of the toxic chemicals in the contaminated water has now become an irrefutable global issue. Therefore, to avoid water pollution, there is an immense need to raise awareness of water management and improve wastewater treatment technologies. To maintain potable water quality, the World health organization (WHO) has set a standard for the permissible limit of various elements in the water for consumption [4, 5].

Water purification techniques, such as adsorption [6], advanced oxidation process (e.g. photocatalysis, Fenton's oxidation) [7], electrocatalysis [8], photoelectrocatalysis [9], membrane filtration [10], biological precipitation [11], flocculation [12], and reserve osmosis [13], have been employed to remove or minimize the water contaminant level in wastewater. A variety of active nanomaterials with a high surface area have been investigated in the water treatment process in various methods. Among several classes of nanomaterials, 2D materials have been appreciated as the most fascinating class of nanomaterials, which can be an ideal candidate for various applications, including wastewater treatment [14]. Graphene is one of the most popular examples of 2D nanomaterials, and since its discovery in 2004 it became the popular choice to host applications [15]. With the continuous research on graphene-based materials, other 2D materials or inorganic analogues of graphene, such as MXene [16], layered double hydroxides [17], Metal–organic frameworks [18], transition metal oxides [19], and transition metal chalcogenides [20], have also become the source of attention to investigate in several fields. Among all, particularly MoS_2-based nanomaterials have also gained significant interest in several applications such as lubrication [21], energy storage [22], catalysis [23, 24], sensors [25] and water treatment [26], which is attributed to its outstanding properties, including excellent mechanical strength, high surface area, low dimension, quantum confinement, and surface defects (Fig. 12.1). Bulk MoS_2 is abundantly available as mineral molybdenite and has been used as catalysts and adsorbents for long [27–29]. However after the development of processes for isolating monolayer or few-layered MoS_2 nanosheets from bulk, with exclusive properties that are precise for the nano-sized material, the study of 2D MoS_2 nanomaterials has gained attention. Since then, the research on synthesis processes, functionalization, tuning and properties of 2D MoS_2 nanomaterials have been came into limelight and became a promising candidate in wastewater treatment [30–33].

Herein, we propose to emphasize the application of 2D MoS_2-based nanomaterials or nanocomposites to remove water contaminants from wastewater using various wastewater treatment techniques. There are several reviews published on water remediation using carbon [34], graphene or graphene-based materials [35, 36], and other 2D materials [37]. Also, the review on the MoS_2 synthesis, and properties, and several applications, especially energy applications, are published [22, 38]. However, a review or chapter focusing on the candidature of 2D MoS_2 in water remediation with a recent update is missing. The detailed mechanism of the MoS_2 materials in water treatment is also discussed. This chapter is dedicated to the application of MoS_2 nanomaterials in cleaning the wastewater through adsorption, photocatalysis, membrane filtration and antibacterial activity (Fig. 12.1) and a perspective on future work for MoS_2 nanomaterials.

12.2 Application of MoS_2 in Wastewater Treatment

Water contamination is a global issue responsible for clean water scarcity and deteriorating human, animal and marine creatures' health. Several techniques have been proposed to clean the wastewater before discharging it into the water bodies or before consumption. With the growing interest of the scientific community towards wastewater treatment to save life on Earth, the application of several nanomaterials has been investigated to clean the water. The approach of nanostructured materials in wastewater remediation offers new dimensions to evaluate, analyse and solve water pollution. Recently, MoS_2 has gained much attention in water remediation due to its unique properties, such as high active surface area, low cost, small band gap and the possibility of surface functionalization. In several studies, MoS_2 and MoS_2-based nanocomposites have been proven as excellent adsorbents and photocatalysts to remove water contaminants. The following sub-section briefly describes the application of MoS_2 and MoS_2-based nanocomposites in wastewater remediation as adsorbent, photocatalyst, membrane, and antibacterial agents.

12.2.1 Adsorption

Adsorption is one of the most explored wastewater treatment techniques, which is widely accepted and lowcost. The presence of plenty of exposed sulphur atoms on the MoS_2 surface provides the platform for the adsorption of cationic water contaminants through strong Lewis acid and base soft–soft interactions [33]. Geng et al. prepared the flower-like nanostructures of MoS_2 nanosheets for the adsorption of cationic (Rhodamine B, RhB) dye, and the adsorption capacity was noticed to be 49.2 $mg.g^{-1}$ [39]. Electrostatic interaction between the cationic dye and negative MoS_2 was found to be the major driven force for the adsorption. To confirm the adsorption behaviour of RhB on MoS_2, FTIR analysis of MoS_2 before and after the adsorption of RhB was performed, which indicates that the intensity of Mo-S peak was reduced and some new vibrational signatures assigned to aromatic rings of RhB has been introduced. This suggests the strong interaction of RhB to the MoS_2 backbone via electrostatic interaction. Further, the application of hierarchical microspheres of MoS_2 nanosheets was also compared for the various cationic (e.g. methylene blue (MB), Rhodamine (Rh) and malachite green (MG)) and anionic dyes (e.g. fuschin acid (FA) and congo red (CR)) adsorption from aqueous medium (Fig. 12.2) [26]. MoS_2 was found to exhibit excellent adsorption capacity for MB followed by others in the following order MB (297 $mg.g^{-1}$) > Rh (216 $mg.g^{-1}$) > MG (204 $mg.g^{-1}$) > FA (183 $mg.g^{-1}$) > CR (146 $mg.g^{-1}$). The high absorption capacity towards cationic dyes was also believed to be the effect of the van der Waals forces and the electrostatic interactions. However, the adsorption of anionic contaminates was only found to be compelled by van der Waals interaction. The adsorption of cationic MB dye on MoS_2 surface was further analysed FTIR spectroscopy. Figure 12.2a shows a FTIR spectra of MB dye, and MoS_2 before and after MB adsorption. The new vibrational signatures on the MB adsorbed MoS_2 are characteristic peaks of MB dye, which confirms the adsorption of MB on MoS_2. Additionally, the Mo-S vibrational peaks remains unchanged in the recovered MoS_2 after MB dye adsorption. Therefore, MoS_2 was also examined for the recyclability and showed an excellent adsorption capacity for 5 adsorption cycles (Fig. 12.2b). The adsorption was followed by Freundlich isotherm model and pseudo second order kinetics. The adsorption capacity of MoS2 for cationic and anionc dyes has shown in Fig. 12.2c.

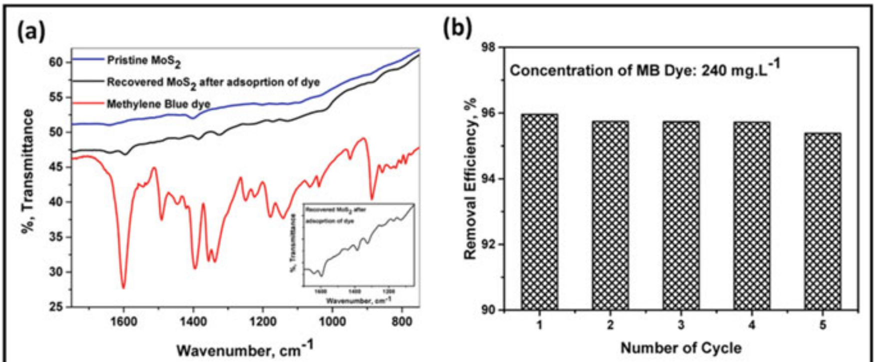

(c)

	Dye	Adsorption Capacity, mg.g-1
Cationic Dye	MB	297
	Rh	216
Anionic Dye	MG	204
	FA	183
	CR	146

Fig. 12.2 **a** FTIR analysis of MB dye, pristine MoS_2 and MoS_2 after MB dye adsorption, **b** recyclability of MoS_2 for MB dye adsorption and **c** adsorption capacity of MoS_2 nanosheets towards cationic and anionic dyes. Reproduced with permission from ref. [26]. Copyright 2016, American Chemical Society

Similar to cationic organic contaminants, MoS_2 is also valuable for removing inorganic heavy metal ions. The adsorption mechanism and all the possible interactions between the heavy metal ions and MoS_2 are nicely explained in parts (a) and (b) of Fig. 12.3 [33, 40]. Several interactions, such as electrostatic interaction, complexation formation, and ion-exchange, help in heavy metal ion adsorption (Fig. 12.3a). Ion-exchange is considered the primary adsorption mechanism for metal adsorption on the MoS_2 surface. Generally, the MoS_2 surface exhibits a negative charge with positive counter ions [40–42], which allows the metal-sulphur bond and results in complexation. Another mechanism is multilayer adsorption which involves the inner layer complex formation (metal sulphur complex formation) and outer layer complex formation (e.g. electrostatic interaction). Another possible adsorption mechanism is the intercalation of metal ions into the MoS_2 nanosheets. Several synthesis routes of MoS_2 nanosheets can introduce defects or widen the interlayer spacing. These spacing are enough to expose the interior sulphur atoms and helps the adsorption of metal ions. For example, Lu et al. followed the one-step hydrothermal route for the MoS_2 nanosheets preparation and achieved to widened the interlayer spacing to 0.94 nm from 0.62 nm (Fig. 12.3b) [40]. This helps in extremely high and fast Hg(I) adsorption (2506 mg.g^{-1}).

However, the adsorption of anionic contaminant on MoS_2 can be improved by the fabrication of MoS_2 with other nanomaterial/polymers as nanocomposite. For

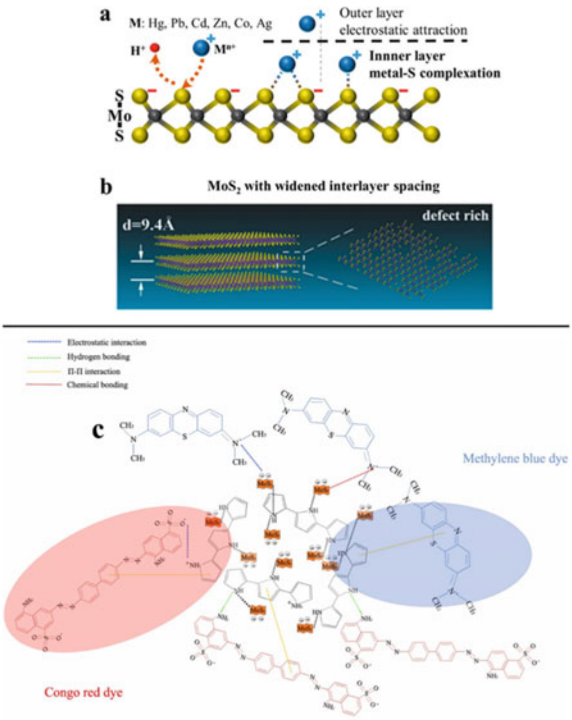

Fig. 12.3 **a** Several plausible adsorption mechanisms for heavy metal ion adsorption on MoS2 nanosheets. Reproduced with permission from ref. [33]. Copyright 2017, American Chemical Society. **b** Schematic representation of widened interlayer spacing in MoS_2 nanosheets. Reproduced with permission from ref. [40]. Copyright 2016, John Wiley and Sons, Inc. **c** Possible adsorption mechanism for the adsorption of CR and MB dye on Ppy@MoS_2. Reproduced with permission from ref. [43]. Copyright 2022, Elsevier Science Ltd.

example, Zhang et al. prepared the polypyrrole functionalized MoS_2 (Ppy@MoS_2) microtubes for MB, RhB, methyl orange (MO) and CR adsorption from wastewater [43]. The resultant composite exhibits a higher specific surface area than pristine MoS_2, which helps in the adsorption of dyes. The composite showed the best adsorption capacity for the anionic dye (CR, 598.79 mg.g^{-1}) than the cationic dye. The high surface area and synergistic effect between MoS_2 and Ppy microtubes is the key to excellent adsorption capacity. The adsorption of CR on Ppy@MOS_2 was driven by several possible interactions, such as electrostatic interaction between the anionic dye and Ppy, π-π interactions between the aromatic rings of the adsorbate and adsorbent, π-π stacking interactions, and hydrogen bonding (Fig. 12.3c). MoS_2 has also been used for the adsorption of oil and organic solvents from the water [44, 45]. Hydrophobic interactions are the major forces for the adsorption of oil and organic solvents on the MoS_2 surface. MoS_2 surface can be engineered into the superhydrophobic (water contact angle from 85° to ~150°) and used as an adsorbent for a wide range of hydrophobic oils and organic solvents [46, 47].

In summary, MoS_2 can be efficiently used as an adsorbent to remove a wide range of water pollutants, preferably cationic contaminants, from wastewater. Electrostatic interaction is considered the major driving force for the adsorption of cationic pollutants on the MoS_2 surface. The Sulphur atom on the MoS_2 surface acts as a Lewis base and exhibits high affinity toward the cationic contaminants. Therefore, the selectivity of MoS_2 is much higher than other adsorbents. However, the functionalization of MoS_2 turned the properties and provided an excellent surface area to adsorb the broad spectrum of all kinds of water contaminants. Other than electrostatic interactions, π–π interaction, hydrogen bonding, metal complexation and van der Waals interaction also participate in the adsorption of water pollutants. Table 12.1 lists examples of various MoS_2-based adsorbent materials for the adsorption of water contaminants with adsorption capacity.

12.2.2 Photocatalysis

Photocatalytic degradation of water contaminant molecules is another promising way to clean wastewater without producing secondary waste. Photocatalytic wastewater treatment is a well-known advanced oxidation process. It exhibits several advantages over other treatment techniques, such as cost-effectiveness, complete degradation or mineralization, simple practice, and mild reaction conditions [70]. 2D MoS_2 nanosheets are one of the exciting photocatalyst candidates due to their excellent charge mobility and high optical absorption characteristics [71–73]. In a typical photocatalysis reaction, a semiconductor material absorbs the photon of energy equal to or more than its band gap energy. It is excited to jump the electrons from the valence band (VB) to the conduction band (CB). This creates holes in the VB, which helps in the oxidation and the excited electrons in the CB help in the reduction to carry out the photocatalytic redox reaction and produce reactive oxygen species (ROS). These ROS species are the active generations that either mineralizes the organic

Table 12.1 Few examples of various MoS_2-based nanoadsorbents with their adsorption capacity for targeted water contaminants

MoS_2 based nanoadsorbent	Targeted water contaminant	Adsorption capacity, $mg.g^{-1}$	References
Magnetic Fe_3O_4/MoS_2	CR	71	[48]
MoS_2/Fe_3O_4	Pb(II) Hg(II)	263.6 428.9	[49]
MoS_2/CeO_2	Pb(II)	333	[50]
MoS_2	RhB	136.99	[51]
Fungus-like MoS_2	CR	285.7	[52]
Hollow MoS_2	MO	41.52	[53]
MoS_2	RhB	365	[54]
C/MoS_2	MO	450	[55]
MoS_2	MB MG RhB FA CR	297 204 216 183 146	[26]
$MoO_3@MoS_2$	RhB	326.8	[56]
FeOCl-MoS_2	MO	1615.11	[57]
MoS2	MB	146.43	[58]
CeO2–MoS_2	Pb(II) Humate	263 218	[59]
MoS_2–rGO	Pb(II) Ni(II)	322 294	[60]
MoS_2@Zeolite-5	Tetracycline (TC)	396.7	[61]
MoS_2	MB MO Co(II) Ni(II)	181.8 102.1 61.7 51.8	[62]
MoS_2@bentonite	Crystal violet (CV)	384.61	[63]
1 T MoS_2 2H-MoS_2	Pb(II) Cu(II) Pb(II) Cu(II)	147.09 82.13 64.16 50.74	[64]
MoS_2 with increased interlayer spacing	Pb(II)	303.04	[65]
Graphene-like layered MoS_2 (g-MoS_2)	Doxycycline (DC)	310	[66]
g-MoS_2 decorated biochar	TC	249.45	[67]
MoS_2/SH-MWCNT	Pb(II) Cd(II)	90 66.6	[68]
MoS_2/Graphene	RhB	285	[69]

molecules or degrade completely. However, one major challenge in photocatalysis is the mobility of charge carriers. The too-small band gap of the semiconductor material is responsible for the quick recombination of the generated electron and hole pairs. Hence, they won't be able to participate in the photocatalytic reaction.

Conversely, too broad-band gap does not absorb the broad spectrum of solar light, thus not appropriate for the photocatalytic response. Bulk MoS_2 exhibit a narrow band gap of ~1.3 eV, allowing the adsorption of most of the solar spectrum. Still, the fast recombination of charge carriers makes a negative impact on its photocatalytic reaction. On exfoliating the bulk MoS_2 to few-layered 2D MoS_2 nanosheets or single-layered MoS_2, the band gap increased enough to improve the life span of charge carriers, adsorption of UV–visible, visible and near-infrared light and consequently improve the photocatalytic reaction [71].

Besides band energy, band edges' position also significantly affects the photochemical reaction. The redox potential of the charge carriers strongly depends on the position of the band edges. For example, the smaller the CB potential, the stronger the reduction capability of photo-generated electrons or the larger the VB potential of semiconductor material, the stronger the oxidative capability of the holes. The band edge positions in the few-layered MoS_2 are more favourable to producing ROS generations than bulk MoS_2. Generally, MoS_2 is explored for the oxidation of water pollutants. In the photo-oxidation of water pollutants, the holes in VB play a vital role. Although the band edge potential of VB for monolayer MoS_2 (1.78 eV) is much higher than the bulk MoS_2 (1.40 eV), but is not sufficient to directly mineralise or decompose the pollutant molecules [74]. Therefore, MoS_2 is majorly used as a co-catalyst in a photocatalyst system to improve the photocatalytic degradation efficiency by increasing the charge mobility and suppressing the charge pair's recombination.

For example, MoS_2 was incorporated with Ag_3PO_4 and TiO_2 to prepare a ternary photocatalyst to degrade the MO, MB dye, and antibiotic Oxytetracycline (OTC) [75]. The ternary photocatalyst ($Ag_3PO_4/TiO_2@MoS_2$) was also compared with the $TiO_2@MoS_2$ for photocatalytic efficiency. Figure 12.4a shows the high-resolution SEM images of the ternary photocatalyst, in which TiO_2 nanofibers (180 nm diameter) are prepared by the electrospinning method and further implemented with a few layers of MoS_2 via a hydrothermal route. Ag_3PO_4 was deposited on the $TiO_2@MoS_2$ surface via chemical deposition to get $Ag_3PO_4/TiO_2@MoS_2$. Additionally, the presence of Ti, Mo, S, Ag and O energy dispersive X-ray spectrometry (EDX) analysis approves the preparation of $Ag_3PO_4/TiO_2@MoS_2$ composite. The prepared materials' optical characteristics and band gap were examined using the UV/vis diffuse reflectance spectrum. The band gap of the ternary photocatalyst was calculated to be 1.85 eV (Fig. 12.4b), which is sufficient to absorb the visible light photon.

Moreover, the ternary composite's light adsorption intensity was higher than binary Ag_3PO_4/MoS_2 and single Ag_3PO_4. The appropriate band gap and excellent light adsorption intensity significantly help the $Ag_3PO_4/TiO_2@MoS_2$ for photocatalytic application. The mechanism of the prepared nanocomposite is also explained in Fig. 12.4c. Under light irradiation, the electrons from Ag_3PO_4 VB jumped to the CB and then transferred to the MoS_2 VB. Meanwhile, the MoS_2 electrons jumped

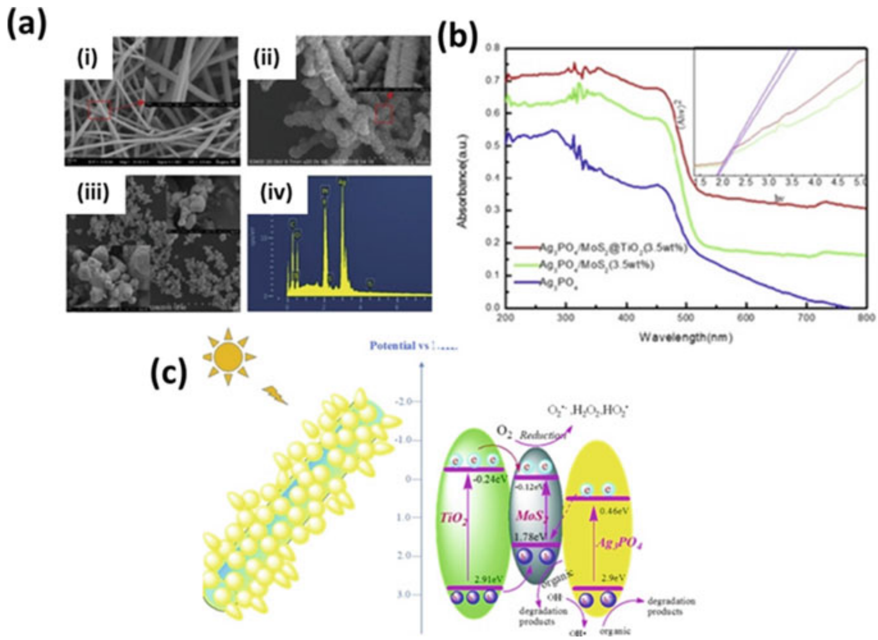

Fig. 12.4 **a** FE-SEM image of $Ag_3PO_4/TiO_2@MoS_2$ photocatalyst ((i) TiO_2 nanofibers, (ii) implantation of MoS_2 on TiO_2 nanofibers ($TiO_2@MoS_2$), (iii) ternary $Ag_3PO_4/TiO_2@MoS_2$ photocatalyst, (iv) EDS of $Ag_3PO_4/TiO_2@MoS_2$ composite), **b** UV–vis absorption graph of ternary $Ag_3PO_4/TiO_2@MoS_2$, binary Ag_3PO_4/MoS_2 and single Ag_3PO_4, and inset graph represents the kubelka–Munk transformed reflectance spectra, to calculate the bandgap values for the binary Ag_3PO4/MoS_2 (3.5 wt%) and ternary $Ag_3PO_4/TiO_2@MoS_2$, and **c** Schematic representation proposed charge mechanism with energy band structure of the ternary $Ag_3PO_4/TiO_2@MoS_2$ composites. Reproduced with permission from ref. [75]. Copyright 2017, Elsevier Science Ltd.

from VB to CB and inhibited the recombination of charge carriers. TiO_2 also trivially participates due to the small amount of UV light adsorption, and TiO_2 VB electrons also migrate to the MoS_2 CB. Subsequently, the TiO_2 fibres act as wire and help transfer the MoS_2 captured electrons in the solution for ROS generations. Also, the VB and CB positions of MoS_2 have higher potential than TiO_2, which helps for holes transfer from TiO_2 VB to MoS_2 VB. These holes can significantly oxidize the organic pollutants. The excellent charge mobility of MoS_2 not only improves the material's photocatalytic efficiency but also inhibits the photocorrosion rate of Ag(I). This improves the cyclic stability of the ternary composite, and only 10% reduction in photocatalytic efficiency was noticed after 10 cycling runs. Therefore, the excellent charge mobility and anti-photocorrosion attitude make MoS_2-based materials encouraging candidates for photocatalysis applications.

Like organic water contaminants, inorganic contaminants were also degraded using MoS_2 photocatalyst. Gao et al., employed the polyaniline (PANI) functionalized MoS_2 for the removal of Cr(VI) as an adsorbent and photocatalyst [76]. Under light irradiation, the PANI-MoS_2 nanocomposite could successfully remove

600 mg.g^{-1} Cr(VI) and photo-catalytically reduce it to Cr(III). The Cr(VI) removal was found to be highly pH dependent. The low pH conditions of the solution favour the reduction of Cr(VI).

In contrast, the reduced $Cr(OH)_3$ can quickly be precipitated on the PANI@MoS_2 surface at high pH conditions and inhibit the active sites. PANI@MoS_2 also perform excellent cyclic recyclability for several cycling runs. Cr(VI) was also photo-catalytically reduced using Fe(0) decorated g-C_3N_4-MoS_2 (GCNFM) nanocomposite [77]. The suitable band edges potential of the photocatalyst favours the photo-reduction of Cr(VI) into Cr(III). Under visible light irradiation, the electrons jumped to the Fe(0) and MoS_2 CB due to appropriate band edge alignments. This enhances the life span of charge carriers and improves the Cr(VI) reduction compared to g-C_3N_4, MoS_2 modified g-C_3N_4 and Fe(0) doped g-C_3N_4. The same photocatalyst also performs effectively for the mineralization of RhB organic dye. Several other MoS_2-modified semiconductor materials have also been examined for the photocatalytic degradation of water contaminants (Table 12.2). In summary, the advantage of photo-stability of MoS_2 than other chalcogenides against oxidation supports the application of MoS_2 in photocatalytic reactions [78]. Additionally, the band structure of a few layered or monolayer MoS_2 helps in the absorption of a broad spectrum of solar light, which is one of the essential demands for the semiconductor material. In the MoS_2-based semiconductor nanocomposite material, MoS_2 actively improve the photo-absorption response, suppress the recombination of charge carriers, providing a platform for the adsorption of contaminant and enhancing the photocatalytic reaction.

12.2.3 Membrane Filtration

The high mechanical strength, excellent thermal stability and antibacterial properties of MoS_2 make it a potent candidate for fabricating membranes with outstanding separation performance. Additionally, MoS_2-based membranes exhibit simultaneous permeability and high selectivity [99, 100], antifouling properties [101, 102] and facilitate multifunctional features [103]. In membrane filtration, the wastewater or contaminated water is passed through an appropriate membrane with specific pore sizes, allowing water to be passed and act as a barrier for contaminants. The filtration can be pressure, thermal, osmosis, and electrical driven. MoS_2 can be used to make nanoporous membranes and layer stacked membrane for wastewater treatment.

Nanoporous membranes are made using a few layers or single-layer MoS_2 nanosheets. The appropriate sizes of nanopores in the membranes are designed to block the passage of unwanted species. Pore characteristics, water filtering species characteristics and external pressure are majorly responsible for the membrane functioning in water purification [104]. The eco-friendly nature with flexible design and high quality of cleaned water through membrane filtration makes the membrane filtration technique popular to clear wastewater. Also, during water transport, the water molecules are connected inside and outside the nanopores by forming single-chain hydrogen bonding, which improves water filtration [105]. Most of the studies

Table 12.2 Few examples of various MoS_2-based nanoadsorbents with their photocatalytic efficiency in degrading the targeted water contaminant

MoS_2 based photocatalyst	Targeted water contaminant	Contaminant		Light source	Degradation efficiency	References
		Concentration $mg.L^{-1}$	Volume mL			
$MoS_2@Fe_3O_4$	RhB MB	10 30	50 50	Visible light	96% 98%	[79]
MoS_2	MB	10	200	Visible light	95.6%	[80]
$BiPO_4$–MoS_2/GR	RhB	5	100	Visible light	93%	[81]
CoS2/MoS_2@Zeolite	TC	200	50	300W Xe lamp, Visible light	96.71	[82]
BiOBr/MoS_2/GO	OTC TC Chlorotetracycline DC	10	25	300W Xe lamp, Visible light	98% 98% 98% 98%	[83]
rGO/MoS_2	MB	12.5	8.5	Simulated solar light	95%	[84]
CeO_2-MoS_2	Cr(VI)	5	20	500W Halogen lamp	99.6%	[85]
CeO_2–ZrO_2@MoS_2	Naproxen (NPX)	10	50	250 W LED lamp, Visible light	96%	[86]
MoS_2/Fe_3O_4	MO	10	50	300W Xe lamp, Visible light	80%	[87]
Fe_7S_8@MoS_2–O	MG Levofloxacin (LVX)	10	50	Xe lamp, Visible light	97.5% 92.7%	[88]
g-C_3N_4/Ag/ MoS_2	RhB	20	100	300W Xe lamp, Visible light	66.47	[89]
$ZnIn_2S_4/MoS_2$	MO	20	10	300W Xe lamp, Visible light	84	[90]
MoS_2/Ag_2CO_3	Lanasol Red 5B RhB Ciprofloxacin Metronidazole	80 40 20 20	40	500W Xe lamp, Visible light	98% 90% 80% 72%	[91]

(continued)

Table 12.2 (continued)

MoS_2 based photocatalyst	Targeted water contaminant	Contaminant		Light source	Degradation efficiency	References
		Concentration $mg.L^{-1}$	Volume mL			
CNT@MoS_2/SnS_2	Cr(VI)	50	50	300W Xe lamp, Visible light	100%	[92]
$SrFe_{12}O_{19}$/MoS_2	MB	20	80	Visible light	97%	[93]
MoS_2/Ag_3PO_4	Ofloxacin (OFL) RhB	10 10	100 100	Visible light Sunlight	79% 100%	[94]
MoS_2/ZnS	OTC	20	100	250 W Hg lamp, UV–visible light	81%	[95]
MoS_2/SnS_2	Cr(VI) MB	120 30	50 50	500W Xe lamp, Visible light	99.9% 96.5%	[96]
$MoS_2 - ZnS$	RhB	5	100	300 W Xe lamp, Visible light	100%	[97]
MoS_2/Bi_5O_7I	Bisphenol A TC Ciprofloxacin	10 20 10	100 100 100	300W Xe lamp, Visible light	99% 78% 40%	[98]

using nanoporous MoS_2-based membranes are used for desalination purposes. The performance of nanoporous MoS_2 membrane is majorly evaluated by theoretical simulation studies, not experimentally.

Heiranian et al. performed the theoretical calculations for the use of nanoporous MoS_2 membranes in water purification, and they concluded that > 88% of ions could easily be filtered using a monolayer MoS_2 membrane of a specific pore area (20 to 60 A^2) [106]. Figure 12.5a shows the typical simulation box consisting of a single-layer MoS_2 nanoporous membrane, a rigid piston (graphene sheet), water and ions. In this simulation box, three pores have been identified: Mo pores, S pores and mixed pores (consisting of Mo and S) (Fig. 12.5b). On comparing monolayer MoS_2 membrane with nanoporous graphene membrane, the water flux was found to be 70% improved with MoS_2 membrane. Figure 12.5c shows the water fluxes through various Mo pores and S pores, mixed pores and graphene sheets with respect to the applied pressure gradient. Among all types of pores in the simulation box, Mo-only pores show the highest water permeation. The mixed pore shows higher water fluxes compared to the graphene nanopores. Figure 12.5d shows the ions rejection through the pores of MoS_2 nanoporous membrane and graphene pores as a function of applied pressure. Ion rejection is lower at a higher pressure and with larger pores. The ion rejection capacity is found to be quite similar for the equivalent areas irrespective of the pore type. This suggested that ion rejection depends on the pore area only and not on the pore type. Figure 12.5e shows that the water filtration rate is also intensely increasing the pore from $\sim$20 to $\sim$50 $Å^2$.

This study suggests that while designing MoS_2 nanoporous membranes, the size and areas of pores are the essential characteristics to be kept in mind. The 0.44 nm or larger (diameter) pore sizes of nanoporous MoS_2 are favourable in wastewater treatment and display a minor energy barrier for water molecules and at the same time, reject the passage of salts [106, 107]. But the much larger diameter of nanopores (>1.05 nm) is not good for separating salts from water as the salt molecules can easily pass through the pores. Therefore, the identical size for the MoS_2 nano-membranes for water purification is suggested as 0.44 to 1.05 nm [33].

However, in MoS_2-based layer stacked membranes, exfoliated MoS_2 membranes are stacked to each other through the vacuum-filtration technique [108]. Efficient sieving of water contaminants (molecules, salt and ions) can be performed at the free layer spacing of capillary width between the stacked 2D MoS_2 nanosheets. The free layer spacing between the nanosheets can be controlled for the high selectivity of water filtration. The advantage of layer-stacked MoS_2 membranes is their high stability in the aqueous medium compared to other layer-stacked membranes, e.g., GO-based membranes [99]. Layer stacked MoS_2 membrane was immersed in water for 3 days to check the water stability, but it didn't swell and maintained its interlayer spacing [99]. This might be due to the absence of any hydrophilic functional group on the MoS_2 membrane surface and the van der Waals force between the stacked nanosheets, which provide the required stability against the redispersion of stacked nanosheets in water.

Additionally, the physical characteristic of 2D MoS_2-based membrane can be tuned or functionalized to boost the water flux and improve the barrier for unwanted

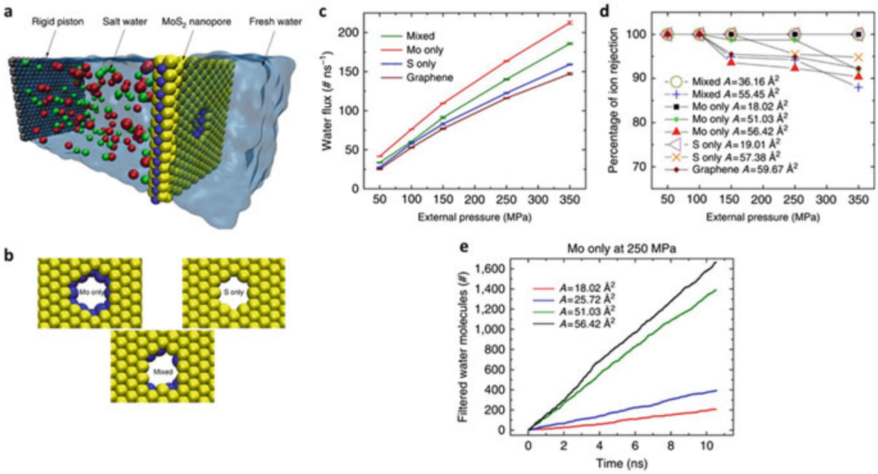

Fig. 12.5 **a** Schematic illustration of simulation box containing a MoS_2 nanosheet (blue colour represents Mo and yellow colour represents S), salt ions (red and green), graphene sheet (dark grey) and water (transparent blue). **b** Left: Pore with Mo only. Right: pore with S only. Bottom: mixed pore consisting of Mo and S. **c** Comparison of Mo-only nanopores, S-only nanopores, mixed nanopores and graphene nanopores for water flux with respect to the applied pressure with similar pore areas. **d** Percentage of ion rejection through several pores of different edge chemistries and pore ares, as a function of the applied pressure. **e** Counts of filtered water molecules through Mo only pores of different pore areas as a function of simulation time at a fixed pressure of 250 MPa. Reproduced with permission from ref. [106]. Copyright 2015, Nature Publications

contaminates [109]. For example, the interlayer spacing of the nanosheets can be modified for selective separation via the intercalation of some species. Lu et al. intercalated the amphiphilic ligand as a cross-linker in layer-stacked MoS_2 to tune the interlayer spacing for water filtration [101]. On the other hand, layer-stacked MoS_2 membranes can also be functionalized by immersing in a dye solution for desalination and nanofiltration [100]. The surface chemistry of the membrane was changed to the functionalized of dye on the surface, which contributed to minimal effect on the interlayer spacing. This helps in the rejection of the ions and salts with high selectivity. Overall 2D MoS_2-based membranes have shown a significant potential for the water treatment. However, the thorough study of MoS_2-based membranes in water purification is still underway as most studies have been performed by theoretical simulations and modellings.

12.2.4 Antibacterial Activity

Wastewater discharge, usually municipal effluents, is the perfect environment for the growth of deadly bacteria, which is a threat to the life of public health [110]. Several bacteria have shown antibiotic resistance, leading scientist to look for other effective alternative antibacterial proxies. Recently, MoS_2 has gained significant attention as an antibacterial agent due to its excellent biocompatibility, large surface area, ease of functionalization, high catalytic activity, cost-effectiveness, and chemical stability [111]. Regardless of its various outstanding characteristics, the application of pristine MoS_2 nanomaterials exhibit some limitations in the biomedical field. Therefore, MoS_2 is functionalized to improve its application as an antibacterial agent. The antibacterial activities of MoS_2 nanosheets have been found to be better than bulk MoS_2 due to the developed photo-response properties of MoS_2-based nanomaterials [112]. MoS_2 nanosheets prevent bacterial multiplication via physical contact, and the sharp ends of nano-architectures may penetrate into the cell wall of bacteria to kill it [113]. However, under the illumination of visible light, the generation of ROS on the MoS_2 surface causes bacterial inactivation, and hence photo-response of MoS_2 nanostructures helps in antibacterial activity. 1 T MoS_2 is considered a better option than 2H MoS_2, as 1 T MoS_2 exhibit higher electrical conductivity and is less resistant to electron migration.

1 T phase of chemically exfoliated MoS_2 (ce-MoS_2) nanosheets was evaluated for antibacterial purpose and compared with raw MoS_2 [115]. The antibacterial properties of ce-MoS_2 were followed by a three-step mechanism: (a) direct physical contact of bacterium-MoS_2, (b) sharp edges of MoS_2 damage the membrane, and (c) MoS_2 creates a disturbance in microbial redox reaction processes. Additionally, ce-MoS_2 is plausible to generate the ROS species under light irradiation, which raw MoS_2 cannot produce and help in high antibacterial activity. ce-MoS_2 also exhibits higher oxidation strength towards the thiols than raw MoS_2, which helps in the death of bacteria. Roy et al. proposed the one-step method to prepare the MoS_2 nanosheets using chitosan (CS-MoS_2). They found that it showed great potential for bactericidal action against both Gram-positive and Gram-negative bacteria [114]. Figure 12.6 shows the different mechanisms for the antibacterial activity of CS-MoS_2 for the bacterial cell death. The antibacterial activity of CS-MoS_2 is a collective action of oxidative stress, membrane damage by penetration and metabolic inactivation.

It is evident that the size and shape considerably affect the properties of the nanomaterials and hence the application efficiency. Xu et al. compared the two morphologies of MoS_2, i.e. nanosheets and nanoflowers, for the antibacterial activity [116]. They concluded that the nanoflowers possessed better antibacterial activity than MoS_2 nanosheets. This might be due to the nanoflower morphology's higher surface area, which provides more space for physical contact and oxidative stress to the bacterial cells. Also, nanoflower morphology shows higher oxidation strength towards the GSH, which helped in bacterial cell death.

12.3 Outlook and Future Perspectives

Among several other 2D materials, the unique properties of MoS_2 have granted its promising candidature in wastewater remediation. MoS_2 and MoS_2-based nanocomposites have been considerably studied as adsorbents, photocatalysts, membranes

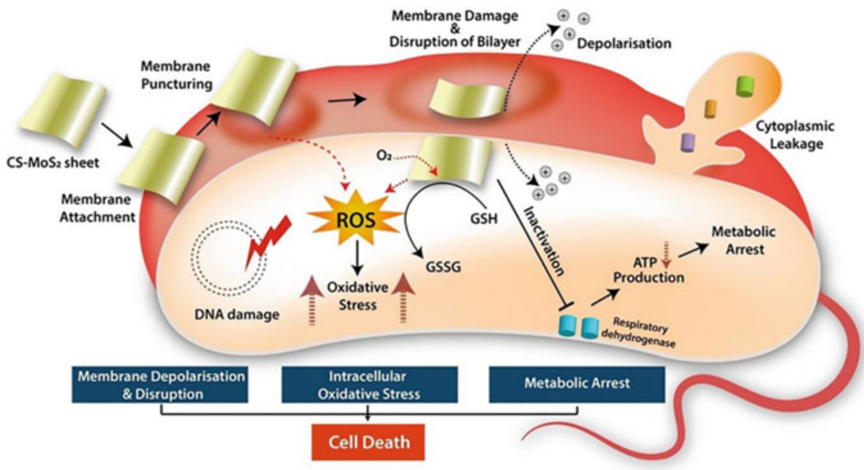

Fig. 12.6 Schematic representation of all the collective proposed mechanisms of antibacterial activity of CS-MoS_2 nanosheets. Reproduced with permission from ref. [114]. Copyright 2019, American Chemical Society

and antibacterial agents to clean wastewater. The application of MoS_2 is extensively explored as an adsorbent and photocatalyst. Despite the fact that an extensive amount of work has been done using MoS_2 in wastewater treatment, there are still a few limitations and daunting challenges for the researchers. MoS_2 surface exhibits a neutral, negative charge, and as an adsorbent material, it is majorly used to remove cationic pollutants from wastewater, which limits its broad application. To remove anionic contaminants, the modification in the MoS_2 as fabrication with other nanoparticles or functionalization with other groups is necessary. This practice usually increases the cost of the water remediation process. Additionally, it is difficult to separate the exfoliated MoS_2 nanosheets from the aqueous medium after the water-contaminant adsorption exercise. This restricts the adsorbent's reusability, increasing costs and producing secondary waste.

MoS_2 and MoS_2-based nanocomposites have also been studied as photocatalysts for the complete degradation or mineralization of water contaminants. The narrow band gap of the MoS_2 allows the absorption of broad solar spectrum photons, which makes it a popular choice. However, simultaneously, the narrow band gap of MoS_2 promotes the rapid recombination of the charge carriers, which is one of the main obstacles to the practical application of MoS_2 as a photocatalyst. To avoid this, researchers use MoS_2 functionalized nanomaterial as a photocatalyst for water decontamination. But the thorough study of band gap structural knowledge, products of water mineralization and photo-stability of the nanocomposite is still lacking. For the advancement in this field, in-depth knowledge and understanding of the photocatalytic mechanism using MoS_2-based nanocomposite is a must. MoS_2-based membranes have shown rapid water transport and a broad range of salt rejection, which is interesting in water treatment. Layer-stacked membranes also demonstrate high water stability, and the filtration process's selectivity can be enhanced by tuning the interlayer spacing of membranes. Therefore, more theoretical and simulation studies are needed for a fundamental understanding of the MoS_2 membrane interlayer and free spacing and the transport of the ions and molecules through the 2D channels [117, 118]. At the same time, the antifouling characteristics of the membrane should be maintained. Another main challenge is the preparation of uniformly and compactly distributed nanopores on the MoS_2 membrane. And at last, but not least, the main concern should be the impact of MoS_2 nanomaterials on the fabrication cost and environment. The synthesis routes of MoS_2 for various water cleaning techniques should be monitored, and the production from lab to pilot scale production should also be targeted.

In order to avoid all these limitations, there are a few suggestions to take into account while designing the MoS_2-based materials for wastewater remediation:

(a) There is a need to improve the adsorption efficiency and selectivity of MoS_2 material for a broad range of water contaminants. To improve the MoS_2 adsorbance competence towards anionic contaminants, it should be smartly functionalized with cost-effective materials. The synthesis route should also avoid the use of any hazardous chemicals.
(b) Dispersion of exfoliated MoS_2 nanostructured material is essential for the enhanced adsorption rate of water contaminant molecules. Homogenously dispersed MoS_2 performs faster adsorption, but at the same time, it faces separation challenges from the treated water. Functionalization of MoS_2 with magnetic materials can avoid this issue. Magnetic MoS_2 material can easily be separated from the treated water using the external magnetic field.
(c) Designing the 3D architecture of 2D MoS_2 nanomaterials is a current research trend to avoid agglomeration and provide more surface area and a porous network for the adsorption of water contaminants.
(d) The study on the band gap structures of MoS_2-based nanocomposites and the types of generated ROS should be performed for a better understanding of the mechanism behind MoS_2-based photocatalytic water decontamination.
(e) The development of multifunctional MoS_2-based membranes can deliver a potential direction for the researcher in future water remediation techniques. Combining the membrane filtration with other wastewater treatment techniques, such as photocatalytic degradation and electrochemical decontamination, using the same MoS_2-based membrane can reduce the water treatment cost and improve the treated water quality.

To conclude, MoS_2-based nano-structural materials nanosheets have shown immense potential for wastewater remediation. However, research using MoS_2 and MoS_2-based nanocomposites in water treatment is still underway. Further research can bring many exciting opportunities and outcomes in wastewater treatment applications.

Acknowledgements The authors would like to acknowledge the funding support from the Department of Science and Innovation (C6A0058), the Council for Scientific and Industrial Research (C6ACH20), and the University of Johannesburg (086310), for their financial support.

References

1. M. Ahmad, M. Yousaf, A. Nasir, I.A. Bhatti, A. Mahmood, X. Fang et al., Porous eleocharis@ MnPE layered hybrid for synergistic adsorption and catalytic biodegradation of toxic Azo dyes from industrial wastewater. Environ. Sci. Technol. **53**, 2161–2170 (2019)
2. S.S. Ray, R. Gusain, N. Kumar, Chapter two - Classification of water contaminants, in *Carbon Nanomaterial-Based Adsorbents for Water Purification*, ed. By S.S Ray, R. Gusain, N. Kumar (Elsevier; 2020), pp. 11–36.
3. R. Gusain, K. Gupta, P. Joshi, O.P. Khatri, Adsorptive removal and photocatalytic degradation of organic pollutants using metal oxides and their composites: A comprehensive review. Adv. Coll. Interface. Sci. **272**, 102009 (2019)
4. M. Kumar, A. Puri, A review of permissible limits of drinking water. Indian J. Occupat. Environment. Med. **16**, 40 (2012)
5. S.K. Sharma, Heavy metals in water: presence, removal and safety: R. Soc. Chem. (2014)
6. S.S. Ray, R. Gusain, N. Kumar, *Carbon Nanomaterial-Based Adsorbents for Water Purification: Fundamentals and Applications* (Elsevier; 2020)
7. D. Kanakaraju, B.D. Glass, M. Oelgemöller, Advanced oxidation process-mediated removal of pharmaceuticals from water: a review. J. Environ. Manage. **219**, 189–207 (2018)
8. H. Rabiee, L. Ge, S. Hu , H. Wang, Z. Yuan, Microtubular electrodes: an emerging electrode configuration for electrocatalysis, bioelectrochemical and water treatment applications. Chem. Eng. J. 138476 (2022)
9. B.O. Orimolade, O.A. Arotiba, Bismuth vanadate in photoelectrocatalytic water treatment systems for the degradation of organics: a review on recent trends. J. Electroanal. Chem. **878**, 114724 (2020)
10. A. Zularisam, A. Ismail, R. Salim, Behaviours of natural organic matter in membrane filtration for surface water treatment—a review. Desalination **194**, 211–231 (2006)
11. A. Magrí, M. Carreras-Sempere, C. Biel, J. Colprim, Recovery of phosphorus from waste water profiting from biological nitrogen treatment: Upstream, concomitant or downstream precipitation alternatives. Agronomy **10**, 1039 (2020)
12. R. Yang, H. Li, M. Huang, H. Yang, A. Li, A review on chitosan-based flocculants and their applications in water treatment. Water Res. **95**, 59–89 (2016)
13. R.H. Hailemariam, Y.C. Woo, M.M. Damtie, B.C. Kim, K.-D. Park, J.-S. Choi, Reverse osmosis membrane fabrication and modification technologies and future trends: A review. Adv. Coll. Interface. Sci. **276**, 102100 (2020)
14. G.H. Jeong, S.P. Sasikala, T. Yun, G.Y. Lee, W.J. Lee, S.O. Kim, Nanoscale assembly of 2D materials for energy and environmental applications. Adv. Mater. **32**, 1907006 (2020)
15. W. Choi, I. Lahiri, R. Seelaboyina, Y.S. Kang, Synthesis of graphene and its applications: a review. Crit. Rev. Solid State Mater. Sci. **35**, 52–71 (2010)
16. Y. Zhang, Y. Yan, H. Qiu, Z. Ma, K. Ruan, J. Gu, A mini-review of MXene porous films: preparation, mechanism and application. J. Mater. Sci. Technol. **103**, 42–49 (2022)
17. P.S. Jijoe, S.R. Yashas, H.P. Shivaraju, Fundamentals, synthesis, characterization and environmental applications of layered double hydroxides: a review. Environ. Chem. Lett. **19**, 2643–2661 (2021)
18. H. Furukawa, K.E. Cordova, M. O'Keeffe, O.M. Yaghi, The chemistry and applications of metal-organic frameworks. Science **341**, 1230444 (2013)

19. K. Gupta, P. Joshi, R. Gusain, O.P. Khatri, Recent advances in adsorptive removal of heavy metal and metalloid ions by metal oxide-based nanomaterials. Coord. Chem. Rev. **445**, 214100 (2021)
20. M. Dai, R. Wang, Synthesis and applications of nanostructured hollow transition metal chalcogenides. Small **17**, 2006813 (2021)
21. S. Kumari, R. Gusain, N. Kumar, O.P. Khatri, PEG-mediated hydrothermal synthesis of hierarchical microspheres of MoS2 nanosheets and their potential for lubrication application. J. Ind. Eng. Chem. **42**, 87–94 (2016)
22. O. Samy, A. El Moutaouakil, A review on MoS2 energy applications: recent developments and challenges. Energies **14**, 4586 (2021)
23. J. Mao, Y. Wang, Z. Zheng, D. Deng, The rise of two-dimensional MoS2 for catalysis. Front. Phys. **13**, 138118 (2018)
24. N. Kumar, S. Kumar, R. Gusain, N. Manyala, S. Eslava, S.S. Ray, Polypyrrole-promoted rGO–MoS2 nanocomposites for enhanced photocatalytic conversion of CO2 and H2O to CO, CH4, and H2 products. ACS Appl. Energy Mater. **3**, 9897–9909 (2020)
25. O. Samy, S. Zeng, M.D. Birowosuto, A. El Moutaouakil, A Review on MoS2 properties, synthesis. Sens. Appl. Chall. Cryst. **11**, 355 (2021)
26. A.T. Massey, R. Gusain, S. Kumari, O.P. Khatri, Hierarchical microspheres of MoS2 nanosheets: efficient and regenerative adsorbent for removal of water-soluble dyes. Ind. Eng. Chem. Res. **55**, 7124–7131 (2016)
27. P. Raybaud, J. Hafner, G. Kresse, S. Kasztelan, H. Toulhoat, Structure, energetics, and electronic properties of the surface of a promoted MoS2 catalyst: an ab initio local density functional study. J. Catal. **190**, 128–143 (2000)
28. L.S. Byskov, J.K. Nørskov, B.S. Clausen, H. Topsøe, DFT calculations of unpromoted and promoted MoS2-based hydrodesulfurization catalysts. J. Catal. **187**, 109–122 (1999)
29. M. Takaoka, N. Takeda, Y. Shimaoka, T. Fujiwara, Removal of mercury in flue gas by the reaction with sulfide compounds. Toxicol. Environ. Chem. **73**, 1–16 (1999)
30. C. Tan, H. Zhang, Two-dimensional transition metal dichalcogenide nanosheet-based composites. Chem. Soc. Rev. **44**, 2713–2731 (2015)
31. H.J. Conley, B. Wang, J.I. Ziegler, R.F. Haglund, S.T. Pantelides, K.I. Bolotin, Bandgap engineering of strained monolayer and bilayer MoS2. Nano Lett. **13**, 3626–3630 (2013)
32. D. Voiry, A. Goswami, R. Kappera, C.D.C.C.E. Silva, D. Kaplan, T. Fujita et al., Covalent functionalization of monolayered transition metal dichalcogenides by phase engineering. Nat. Chem. **7**, 45–49 (2015)
33. Z. Wang, B. Mi, Environmental applications of 2D molybdenum disulfide (MoS2) nanosheets. Environ. Sci. Technol. **51**, 8229–8244 (2017)
34. R. Gusain, N. Kumar, S.S. Ray, Recent advances in carbon nanomaterial-based adsorbents for water purification. Coord. Chem. Rev. **405**, 213111 (2020)
35. G.Z. Kyzas, E.A. Deliyanni, K.A. Matis, Graphene oxide and its application as an adsorbent for wastewater treatment. J. Chem. Technol. Biotechnol. **89**, 196–205 (2014)
36. A. Jilani, M.H.D. Othman, M.O. Ansari, S.Z. Hussain, A.F. Ismail, I.U. Khan, Graphene and its derivatives: synthesis, modifications, and applications in wastewater treatment. Environ. Chem. Lett. **16**, 1301–1323 (2018)
37. S. Dervin, D.D. Dionysiou, S.C. Pillai, 2D nanostructures for water purification: graphene and beyond. Nanoscale **8**, 15115–15131 (2016)
38. H. Wang, C. Li, P. Fang, Z. Zhang, J.Z. Zhang, Synthesis, properties, and optoelectronic applications of two-dimensional MoS 2 and MoS 2-based heterostructures. Chem. Soc. Rev. **47**, 6101–6127 (2018)
39. X. Wang, J. Ding, S. Yao, X. Wu, Q. Feng, Z. Wang et al., High supercapacitor and adsorption behaviors of flower-like MoS 2 nanostructures. J. Mater. Chem. A. **2**, 15958–15963 (2014)
40. K. Ai, C. Ruan, M. Shen, L. Lu, MoS2 nanosheets with widened interlayer spacing for high-efficiency removal of mercury in aquatic systems. Adv. Func. Mater. **26**, 5542–5549 (2016)

41. S.S. Chou, M. De, J. Kim, S. Byun, C. Dykstra, J. Yu et al., Ligand conjugation of chemically exfoliated MoS2. J. Am. Chem. Soc. **135**, 4584–4587 (2013)
42. A.E. Gash, A.L. Spain, L.M. Dysleski, C.J. Flaschenriem, A. Kalaveshi, P.K. Dorhout et al., Efficient recovery of elemental mercury from Hg (II)-contaminated aqueous media using a redox-recyclable ion-exchange material. Environ. Sci. Technol. **32**, 1007–1012 (1998)
43. Y. Zhang, S. He, Y. Zhang, Y. Feng, Z. Pan, M. Zhang, Facile synthesis of PPy@ MoS2 hollow microtubes for removal of cationic and anionic dyes in water treatment. Colloids Surf., A **632**, 127765 (2022)
44. T. Krasian, W. Punyodom, P. Worajittiphon, A hybrid of 2D materials (MoS2 and WS2) as an effective performance enhancer for poly (lactic acid) fibrous mats in oil adsorption and oil/water separation. Chem. Eng. J. **369**, 563–575 (2019)
45. J. Joy, J. Abraham, J. Sunny, J. Mathew, S.C. George, Hydrophobic, superabsorbing materials from reduced graphene oxide/MoS2 polyurethane foam as a promising sorbent for oil and organic solvents. Polym. Testing **87**, 106429 (2020)
46. X. Gao, X. Wang, X. Ouyang, C. Wen, Flexible superhydrophobic and superoleophilic MoS2 sponge for highly efficient oil-water separation. Sci. Rep. **6**, 1–8 (2016)
47. P.K. Chow, E. Singh, B.C. Viana, J. Gao, J. Luo, J. Li et al., Wetting of mono and few-layered WS2 and MoS2 films supported on Si/SiO2 substrates. ACS Nano **9**, 3023–3031 (2015)
48. H.J. Song, S. You, X.H. Jia, J. Yang, MoS2 nanosheets decorated with magnetic Fe3O4 nanoparticles and their ultrafast adsorption for wastewater treatment. Ceram. Int. **41**, 13896–13902 (2015)
49. Z. Wang, J. Zhang, T. Wen, X. Liu, Y. Wang, H. Yang et al., Highly effective remediation of Pb(II) and Hg(II) contaminated wastewater and soil by flower-like magnetic MoS2 nanohybrid. Sci. Total Environ. **699**, 134341 (2020)
50. S. Tong, H. Deng, L. Wang, T. Huang, S. Liu, J. Wang, Multi-functional nanohybrid of ultrathin molybdenum disulfide nanosheets decorated with cerium oxide nanoparticles for preferential uptake of lead (II) ions. Chem. Eng. J. **335**, 22–31 (2018)
51. Z. Li, X. Meng, Z. Zhang, Equilibrium and kinetic modelling of adsorption of Rhodamine B on MoS2. Mater. Res. Bull. **111**, 238–244 (2019)
52. H. Song, S. You, X. Jia, Synthesis of fungus-like MoS2 nanosheets with ultrafast adsorption capacities toward organic dyes. Appl. Phys. A **121**, 541–548 (2015)
53. Y. Wu, M. Su, J. Chen, Z. Xu, J. Tang, X. Chang et al., Superior adsorption of methyl orange by h-MoS2 microspheres: Isotherm, kinetics, and thermodynamic studies. Dyes Pigm. **170**, 107591 (2019)
54. X. Xiao, Y. Wang, B. Cui, X. Zhang, D. Zhang, X. Xu, Preparation of MoS2 nanoflowers with rich active sites as an efficient adsorbent for aqueous organic dyes. New J. Chem. **44**, 4558–4567 (2020)
55. H. Yang, H. Yuan, Q. Hu, W. Liu, D. Zhang, Synthesis of mesoporous C/MoS2 for adsorption of methyl orange and photocatalytic sterilization. Appl. Surf. Sci. **504**, 144445 (2020)
56. J. Chen, Y. Liao, X. Wan, S. Tie, B. Zhang, S. Lan et al., A high performance MoO3@MoS2 porous nanorods for adsorption and photodegradation of dye. J. Solid State Chem. **291**, 121652 (2020)
57. X. Liu, W. Zhang, L. Mao, Y. Yin, L. Hu, Synthesis of FeOCl-MoS2 with excellent adsorption performance for methyl orange. J. Mater. Sci. **56**, 6704–6718 (2021)
58. X.-Q. Qiao, F.-C. Hu, F.-Y. Tian, D.-F. Hou, D.-S. Li, Equilibrium and kinetic studies on MB adsorption by ultrathin 2D MoS2 nanosheets. RSC Adv. **6**, 11631–11636 (2016)
59. R. Li, H. Deng, X. Zhang, J.J. Wang, M.K. Awasthi, Q. Wang et al., High-efficiency removal of Pb(II) and humate by a CeO2–MoS2 hybrid magnetic biochar. Biores. Technol. **273**, 335–340 (2019)
60. M.J. Aghagoli, F. Shemirani, Hybrid nanosheets composed of molybdenum disulfide and reduced graphene oxide for enhanced solid phase extraction of Pb(II) and Ni(II). Microchim. Acta **184**, 237–244 (2017)
61. J. Liu, H. Lin, Y. Dong, Y. He, W. Liu, Y. Shi, The effective adsorption of tetracycline onto MoS2@Zeolite-5: Adsorption behavior and interfacial mechanism. J. Environ. Chem. Eng. **9**, 105912 (2021)

62. Y. Li, C. Tang, L. Yang, Y. Sun, W. Ju, Integrated roles of MoS2 nanosheets for water treatment and polymer flame retardant. Arab. J. Sci. Eng. **46**, 6753–6763 (2021)
63. M.K. Uddin, F. Mashkoor, I.M. AlArifi, A. Nasar, Simple one-step synthesis process of novel MoS2@bentonite magnetic nanocomposite for efficient adsorption of crystal violet from aqueous solution. Mater. Res. Bull. **139**, 111279 (2021)
64. J. Luo, K. Fu, M. Sun, K. Yin, D. Wang, X. Liu et al., Phase-mediated heavy metal adsorption from aqueous solutions using two-dimensional layered MoS2. ACS Appl. Mater. Interfaces. **11**, 38789–38797 (2019)
65. N. Kumar, E. Fosso-Kankeu, S.S. Ray, Achieving controllable MoS2 nanostructures with increased interlayer spacing for efficient removal of Pb(II) from aquatic systems. ACS Appl. Mater. Interfaces. **11**, 19141–19155 (2019)
66. Y. Chao, W. Zhu, X. Wu, F. Hou, S. Xun, P. Wu et al., Application of graphene-like layered molybdenum disulfide and its excellent adsorption behavior for doxycycline antibiotic. Chem. Eng. J. **243**, 60–67 (2014)
67. Z. Zeng, S. Ye, H. Wu, R. Xiao, G. Zeng, J. Liang et al., Research on the sustainable efficacy of g-MoS2 decorated biochar nanocomposites for removing tetracycline hydrochloride from antibiotic-polluted aqueous solution. Sci. Total Environ. **648**, 206–217 (2019)
68. R. Gusain, N. Kumar, E. Fosso-Kankeu, S.S. Ray, Efficient removal of Pb(II) and Cd(II) from industrial mine water by a hierarchical MoS2/SH-MWCNT nanocomposite. ACS Omega **4**, 13922–13935 (2019)
69. C. Wang, J. Jin, Y. Sun, J. Yao, G. Zhao, Y. Liu, In-situ synthesis and ultrasound enhanced adsorption properties of MoS2/graphene quantum dot nanocomposite. Chem. Eng. J. **327**, 774–782 (2017)
70. M.R. Hoffmann, S.T. Martin, W. Choi, D.W. Bahnemann, Environmental applications of semiconductor photocatalysis. Chem. Rev. **95**, 69–96 (1995)
71. Y.J. Yuan, H.W. Lu, Z.T. Yu, Z.G. Zou, Noble-metal-free molybdenum disulfide cocatalyst for photocatalytic hydrogen production. Chemsuschem **8**, 4113–4127 (2015)
72. X. Jin, X. Fan, J. Tian, R. Cheng, M. Li, L. Zhang, MoS 2 quantum dot decorated gC 3 N 4 composite photocatalyst with enhanced hydrogen evolution performance. RSC Adv. **6**, 52611–52619 (2016)
73. M. Ntakadzeni, W.W. Anku, N. Kumar, P.P. Govender, L. Reddy, PEGylated MoS2 Nanosheets: a dual functional photocatalyst for photodegradation of organic dyes and photoreduction of chromium from aqueous solution **2019**, 11 (2019)
74. N. Singh, G. Jabbour, U. Schwingenschlögl, Optical and photocatalytic properties of two-dimensional MoS2. Europ. Phys. J. B. **85**, 1–4 (2012)
75. N. Shao, J. Wang, D. Wang, P. Corvini, Preparation of three-dimensional Ag3PO4/TiO2@ MoS2 for enhanced visible-light photocatalytic activity and anti-photocorrosion. Appl. Catal. B **203**, 964–978 (2017)
76. Y. Gao, C. Chen, X. Tan, H. Xu, K. Zhu, Polyaniline-modified 3D-flower-like molybdenum disulfide composite for efficient adsorption/photocatalytic reduction of Cr (VI). J. Colloid Interface Sci. **476**, 62–70 (2016)
77. X. Wang, M. Hong, F. Zhang, Z. Zhuang, Y. Yu, Recyclable nanoscale zero valent iron doped g-C3N4/MoS2 for efficient photocatalysis of RhB and Cr(VI) driven by visible light. ACS Sustain. Chem. Eng. **4**, 4055–4063 (2016)
78. T. Thurston, J. Wilcoxon, Photooxidation of organic chemicals catalyzed by nanoscale MoS2. J. Phys. Chem. B **103**, 11–17 (1999)
79. Q. Wang, S. Dong, D. Zhang, C. Yu, J. Lu, D. Wang et al., Magnetically recyclable visible-light-responsive MoS2@Fe3O4 photocatalysts targeting efficient wastewater treatment. J. Mater. Sci. **53**, 1135–1147 (2018)
80. B. Sheng, J. Liu, Z. Li, M. Wang, K. Zhu, J. Qiu et al., Effects of excess sulfur source on the formation and photocatalytic properties of flower-like MoS2 spheres by hydrothermal synthesis. Mater. Lett. **144**, 153–156 (2015)
81. H. Lv, Y. Liu, H. Tang, P. Zhang, J. Wang, Synergetic effect of MoS2 and graphene as cocatalysts for enhanced photocatalytic activity of BiPO4 nanoparticles. Appl. Surf. Sci. **425**, 100–106 (2017)

82. J. Liu, H. Lin, Y. He, Y. Dong, Gueret yadiberet menzembere ER. Novel CoS2/MoS2@Zeolite with excellent adsorption and photocatalytic performance for tetracycline removal in simulated wastewater. J. Cleaner Product. **260**, 121047 (2020)
83. Y. Li, Z. Lai, Z. Huang, H. Wang, C. Zhao, G. Ruan et al., Fabrication of BiOBr/MoS2/graphene oxide composites for efficient adsorption and photocatalytic removal of tetracycline antibiotics. Appl. Surf. Sci. **550**, 149342 (2021)
84. S. Cravanzola, F. Cesano, G. Magnacca, A. Zecchina, D. Scarano, Designing rGO/MoS2 hybrid nanostructures for photocatalytic applications. RSC Adv. **6**, 59001–59008 (2016)
85. H. Wang, F. Wen, X. Li, X. Gan, Y. Yang, P. Chen et al., Cerium-doped MoS2 nanostructures: efficient visible photocatalysis for Cr(VI) removal. Sep. Purif. Technol. **170**, 190–198 (2016)
86. K. Talukdar, K. Saravanakumar, Y. Kim, A. Fayyaz, G. Kim, Y. Yoon et al., Rational construction of CeO2–ZrO2@MoS2 hybrid nanoflowers for enhanced sonophotocatalytic degradation of naproxen: mechanisms and degradation pathways. Compos. B Eng. **215**, 108780 (2021)
87. X. Lin, X. Wang, Q. Zhou, C. Wen, S. Su, J. Xiang et al., Magnetically recyclable MoS2/Fe3O4 hybrid composite as visible light responsive photocatalyst with enhanced photocatalytic performance. ACS Sustain. Chem. Eng. **7**, 1673–1682 (2019)
88. S. Wang, M.-R. Chen, S.-B. Shen, C.-H. Cheng, A.-J. Cai, A.-J. Song et al., Bifunctionalized Fe7S8@MoS2–O core-shell with efficient photocatalytic activity based on internal electric field. J. Cleaner Product. **335**, 130375 (2022)
89. D. Lu, H. Wang, X. Zhao, K.K. Kondamareddy, J. Ding, C. Li et al., Highly efficient visible-light-induced photoactivity of Z-scheme g-C3N4/Ag/MoS2 ternary photocatalysts for organic pollutant degradation and production of hydrogen. ACS Sustain. Chem. Eng. **5**, 1436–1445 (2017)
90. W.Y. Lim, M. Hong, G.W. Ho, In situ photo-assisted deposition and photocatalysis of ZnIn2S4/transition metal chalcogenides for enhanced degradation and hydrogen evolution under visible light. Dalton Trans. **45**, 552–560 (2016)
91. S. Fu, W. Yuan, Y. Yan, H. Liu, X. Shi, F. Zhao et al., Highly efficient visible-light photoactivity of Z-scheme MoS2/Ag2CO3 photocatalysts for organic pollutants degradation and bacterial inactivation. J. Environ. Manage. **252**, 109654 (2019)
92. R. Dong, Y. Zhong, D. Chen, N. Li, Q. Xu, H. Li et al., Morphology-controlled fabrication of CNT@MoS2/SnS2 nanotubes for promoting photocatalytic reduction of aqueous Cr(VI) under visible light. J. Alloy. Compd. **784**, 282–292 (2019)
93. S. Chen, Y. Di, H. Li, M. Wang, B. Jia, R. Xu et al., Efficient photocatalytic dye degradation by flowerlike MoS2/SrFe12O19 heterojunction under visible light. Appl. Surf. Sci. **559**, 149855 (2021)
94. J. Piriyanon, T. Chankhanittha, S. Youngme, K. Hemavibool, S. Nijpanich, S. Juabrum et al., Fabrication of MoS2/Ag3PO4 S-scheme photocatalyst for visible-light-active degradation of organic dye and antibiotic in wastewater. J. Mater. Sci.: Mater. Electron. **32**, 19798–19819 (2021)
95. R. Gusain, N. Kumar, F. Opoku, P.P. Govender, S.S. Ray, MoS2 nanosheet/ZnS composites for the visible-light-assisted photocatalytic degradation of oxytetracycline. ACS Appl. Nano Mater. **4**, 4721–4734 (2021)
96. T. Qiang, L. Chen, Y. Xia, X. Qin, Dual modified MoS2/SnS2 photocatalyst with Z-scheme heterojunction and vacancies defects to achieve a superior performance in Cr (VI) reduction and dyes degradation. J. Clean. Prod. **291**, 125213 (2021)
97. S.V.P. Vattikuti, C. Byon, S. Jeon, Enhanced photocatalytic activity of ZnS nanoparticles loaded with MoS2 nanoflakes by self-assembly approach. Phys. B **502**, 103–112 (2016)
98. S. Yin, R. Chen, M. Ji, Q. Jiang, K. Li, Z. Chen et al., Construction of ultrathin MoS2/Bi5O7I composites: Effective charge separation and increased photocatalytic activity. J. Colloid Interface Sci. **560**, 475–484 (2020)
99. Z. Wang, Q. Tu, S. Zheng, J.J. Urban, S. Li, B. Mi, Understanding the aqueous stability and filtration capability of MoS2 membranes. Nano Lett. **17**, 7289–7298 (2017)
100. W. Hirunpinyopas, E. Prestat, S.D. Worrall, S.J. Haigh, R.A. Dryfe, M.A. Bissett, Desalination and nanofiltration through functionalized laminar MoS2 membranes. ACS Nano **11**, 11082–11090 (2017)

101. X. Lu, U.R. Gabinet, C.L. Ritt, X. Feng, A. Deshmukh, K. Kawabata et al., Relating selectivity and separation performance of lamellar two-dimensional molybdenum disulfide (MoS2) membranes to nanosheet stacking behavior. Environ. Sci. Technol. **54**, 9640–9651 (2020)
102. M.S. Sri Abirami Saraswathi, D. Rana, P. Vijayakumar, S. Alwarappan, A. Nagendran, Tailored PVDF nanocomposite membranes using exfoliated MoS2 nanosheets for improved permeation and antifouling performance. New J. Chem. **41**, 14315–14324 (2017)
103. L. Zhang, X. He, Q. Zhou, X. Hu, Fabrication of 1T-MoS2 nanosheets and the high-efficiency removal of toxic metals in aquatic systems: performance and mechanisms. Chem. Eng. J. **386**, 123996 (2020)
104. I. Singha, P.K. Mishrab, Nano-membrane filtration a novel application of nanotechnology for waste water treatment. Mater. Today: Proc. **29**, 327–332 (2020)
105. J. Kou, J. Yao, L. Wu, X. Zhou, H. Lu, F. Wu et al., Nanoporous two-dimensional MoS2 membranes for fast saline solution purification. Phys. Chem. Chem. Phys. **18**, 22210–22216 (2016)
106. M. Heiranian, A.B. Farimani, N.R. Aluru, Water desalination with a single-layer MoS2 nanopore. Nat. Commun. **6**, 8616 (2015)
107. J. Kou, J. Yao, L. Wu, X. Zhou, H. Lu, F. Wu et al., Nanoporous two-dimensional MoS 2 membranes for fast saline solution purification. Phys. Chem. Chem. Phys. **18**, 22210–22216 (2016)
108. L. Sun, H. Huang, X. Peng, Laminar MoS 2 membranes for molecule separation. Chem. Commun. **49**, 10718–10720 (2013)
109. J. Sun, Y. Chen, C. Hu, H. Liu, J. Qu, Modulation of cation trans-membrane transport in GO-MoS2 membranes through simultaneous control of interlayer spacing and ion-nanochannel interactions. Chemosphere **222**, 156–164 (2019)
110. S.A. Wakelin, M.J. Colloff, R.S. Kookana, Effect of wastewater treatment plant effluent on microbial function and community structure in the sediment of a freshwater stream with variable seasonal flow. Appl. Environ. Microbiol. **74**, 2659–2668 (2008)
111. A. Sethulekshmi, A. Saritha, K. Joseph, A.S. Aprem, S.B. Sisupal, MoS2 based nanomaterials: Advanced antibacterial agents for future. J. Control. Release **348**, 158–185 (2022)
112. X. Tian, Y. Sun, S. Fan, M.D. Boudreau, C. Chen, C. Ge et al., Photogenerated charge carriers in molybdenum disulfide quantum dots with enhanced antibacterial activity. ACS Appl. Mater. Interfaces. **11**, 4858–4866 (2019)
113. M. Zhang, K. Wang, S. Zeng, Y. Xu, W. Nie, P. Chen et al., Visible light-induced antibacterial effect of MoS2: effect of the synthesis methods. Chem. Eng. J. **411**, 128517 (2021)
114. S. Roy, A. Mondal, V. Yadav, A. Sarkar, R. Banerjee, P. Sanpui et al., Mechanistic insight into the antibacterial activity of chitosan exfoliated MoS2 nanosheets: membrane damage, metabolic inactivation, and oxidative stress. ACS Appl. Bio Mater. **2**, 2738–2755 (2019)
115. X. Yang, J. Li, T. Liang, C. Ma, Y. Zhang, H. Chen et al., Antibacterial activity of two-dimensional MoS2 sheets. Nanoscale **6**, 10126–10133 (2014)
116. Q. Xu, P. Zhu, J. Zhang, Y. Liu, L. Cai, H. Jiang et al., Electrochemical formation of distinct nanostructured MoS2 with altered antibacterial activity. Mater. Lett. **271**, 127809 (2020)
117. Y. Xiang, Y. Liu, B. Mi, Y. Leng, Hydrated polyamide membrane and its interaction with alginate: a molecular dynamics study. Langmuir **29**, 11600–11608 (2013)
118. Y. Xiang, Y. Liu, B. Mi, Y. Leng, Molecular dynamics simulations of polyamide membrane, calcium alginate gel, and their interactions in aqueous solution. Langmuir **30**, 9098–9106 (2014)